IBGM
GIF EVALUATIN - 2015
IRAQI BULLETIN OF GEOLOGY AND MINING
Global Impact Factor
0.744

*Iraqi Bulletin of Geology and Mining* *Vol.12, No.2, 2016* *p 47 – 62*

# GEOELECTRICAL STUDY OF MIDDLE MIOCENE – RECENT SEQUENCES SOUTHWEST KARBALA CITY, CENTRAL IRAQ

**Hayder A. Al-Bahadily[1], Sabah O. Abdulqadir[2] and Andrew J. Long[3]**

Received: 24/ 07/ 2015, Accepted: 16/ 02/ 2016
Key words: Geoelectrical study, Groundwater exploration, Electrical survey, Vertical Electrical Sounding (VES), Groundwater aquifer, Electrical anisotropy

## ABSTRACT

The study area is characterized by arid climate, covering some 160 $Km^2$ of dissected Middle Pleistocene alluvial fan and lies 6 Km southwest of Karbala City. Tectonically, it lies along Abu Jir Fault on the western margin of the Mesopotamia Foredeep. This work aims to study and analyze the Middle Miocene – Recent stratigraphic sequence utilizing Vertical Electrical Sounding (VES) in order to determine the possible presence of groundwater aquifers. The resultant type curves include a variety of earth models, ranging from 3 to 8 layers. Two contour maps of groundwater are presented with average aquifer depth of 38.1 m, and average resistivity of 11.4 Ωm. Analysis of the electrical anisotropy coefficient for the sequences overlying the aquifer indicates that both the resistivity – anisotropy, and thickness – anisotropy relationships follow polynomial functions. Furthermore, the anisotropy coefficient is more sensitive to resistivity variation than bed thickness variation. The occurrence of water saturated clay beds and marls (i.e. high conductivity) within a stratigraphic sequence render the electrical medium anisotropic. The map of the electrical anisotropy indicates that the high values in the northern half of the study area may be attributed to the presence of claystone beds. A lack of gypcrete alteration in this area, coupled with low topographic relief supports the hypothesis that the flow of rain water saturates the underlying claystone beds.

Results of drilling show the aquifer to be confined, and overlain by impermeable dry claystone beds, of relatively high resistivity. However in the northern region, the shallow (more porous) upper units of the same claystone sequence are water saturated (by rainwater infiltration) giving rise to similar low resistivity values to the aquifer.

It is concluded that the geoelectrical models are highly affected by the tectonic and structural setting of the study area, as indicated by the depth offsets of vertically contiguous resistivity responses. In addition, the marl beds, which underlie the aquifer bearing zone, exhibit a negligibly small resistivity contrast with the aquifer, such that in many models its response is integrated with the aquifer as a single electrical layer. The resultant isopach maps of aeolian sand (top soil) and gypcrete indicate the eastern and southeastern parts of the study area to be most useful for agricultural development.

[1] Chief Geophysicist, Iraq Geological Survey, P.O. Box 986, Baghdad, Iraq.
[2] Senior Chief Geophysicist, Iraq Geological Survey, P.O. Box 986, Baghdad, Iraq.
[3] Consultant geoscientist, UK.

# دراسة جيوكهربائية لتتابعات المايوسين الأوسط – العصر الحديث للمنطقة الواقعة جنوب غرب مدينة كربلاء، وسط العراق

**حيدر عدنان البهادلي، صباح عمر عبد القادر و آندرو جيمس لونگ**

**المستخلص**

تقع منطقة الدراسة، البالغة مساحتها 160 كم$^2$، على بعد 6 كم بالاتجاه الجنوبي الغربي من مدينة كربلاء، وتمثل جزء من مروحة غرينية كبيرة تكونت خلال عصر البلايستوسين المبكر – الأوسط. كما وتقع، من الناحية البنيوية، أقصى الغرب من نطاق حوض وادي الرافدين متأثرة بنظام فوالق أبو جير. وهي تمتاز بمناخ صحراوي جاف. إن الهدف من العمل الحالي هو دراسة وتحليل التتابعات الطباقية للفترة من عمر المايوسين الأوسط الى العصر الحديث وتحديد عمق الخزان المائي الجوفي ضمن هذا التتابع وذلك باستخدام تقنية المسح الكهربائي العمودي (ترتيب شلمبرجر).

قدمت عدد من الخرائط على مستوى المنطقة من ضمنها خريطة تبين عمق الخزان الجوفي (بلغ معدل عمقه38.1 م)، وأخرى تبين توزيع قيم المقاومة النوعية للخزان (معدل المقاومة النوعية للخزان 11.4 أوم.م). تبين من خلال دراسة معامل عدم تساوي الخواص بدلالة الإتجاه للتتابعات الطباقية التي تعلو الخزان، إن هذا المعامل يتأثر بشكل كبير بالتغيرات الحاصلة في قيمة المقاومة الكهربائية لطبقة ما أكثر من تأثره بتغيرات سمك هذه الطبقة وان العلاقة البيانية بين هذا المعامل والمقاومة النوعية وكذا بينه وبين سمك الطبقة تخضع لدوال رياضية متعددة الحدود. كما تبين ان القيم العالية له في النصف الشمالي من الممكن ان ترتبط بوجود الطبقة الطينية المشبعة بالمياه ضمن الجزء العلوي من التتابع الطباقي. من المعتقد ان يعود سبب التشبع المائي لهذه الطبقة الى غياب الطبقة الجبسية العليا (غير النفاذة) وأيضا الى الوضع الطوبوغرافي اللذان ساعدا في تجمع وزيادة ترشيح المياه المغذية للطبقة الطينية المذكورة. لقد بينت نتائج الحفر اللاحقة ان تتابع الصخور الفتاتية يظهر كطبقة كهربائية واحدة في التتابع الكهربائي بينما تنفصل طبقة الطين أو الطفل الى طبقتين كهربائيتين، كما بينت ان القيمة الواطئة للمقاومة النوعية الواقعة في الجزء العلوي من التتابع الكهربائي والمقاربة لتلك العائدة للخزان الجوفي تعود الى وجود الطبقة الطينية. ان الصورة الجيوكهربائية للمنطقة من الممكن ان تكون متأثرة وبشكل واضح بالوضع التركيبي والبنيوي لها. كما ان طبقة الطفل التي تحد الخزان من الأسفل لها مقاومة نوعية مقاربة لتلك التي للخزان، وفي الكثير من الحالات، فإن هذه الطبقة تندمج مع الخزان الجوفي لتظهر كطبقة كهربائية واحدة في التتابع الكهربائي. ولقد تبين أيضا، من خلال خارطتي السماكة للطبقتين العلويتين، ان الجزئين الوسطي الشرقي والجنوبي الشرقي من المنطقة هما الأنسب للاستخدام الزراعي.

## INTRODUCTION

The electrical technique has some limitations that render the method inapplicable, most notably where low resistivity contrasts exists between the surrounding medium and the target (Al-Azawi, 1997 and Abdullahi *et al*., 2014). Conversely, good results are acquired when the resistivity of the target is distinctive and measurable throughout the study area.

The study area is defined by the following coordinates (Fig.1); 32° 25' to 32°35' N and 43° 55' to 44° 00' E. The area is located in a large alluvial fan, developed during Early – Middle Pleistocene times (Al-Khatib, 1988) (Fig.1). The relief is generally flat with gently rolling slopes dissected by sparse, shallow valleys, gullies and channels offering poor surface drainage. The drainage pattern draws surface water from the southwest towards the northeast (Fig.1).

The climate is arid within essentially a desert environment. It is characterized by hot and dry summers and relatively cold winters with low rainfall. Therefore, exploration for groundwater resources is essential for the sustainment and development of the agricultural sector. The study area has a cover of recent Quaternary sediment and lacks any existing borehole information. The aim of the study is to locate groundwater aquifers. It also aims to study and analyze the Middle Miocene – Recent stratigraphic sequence by using VES technique.

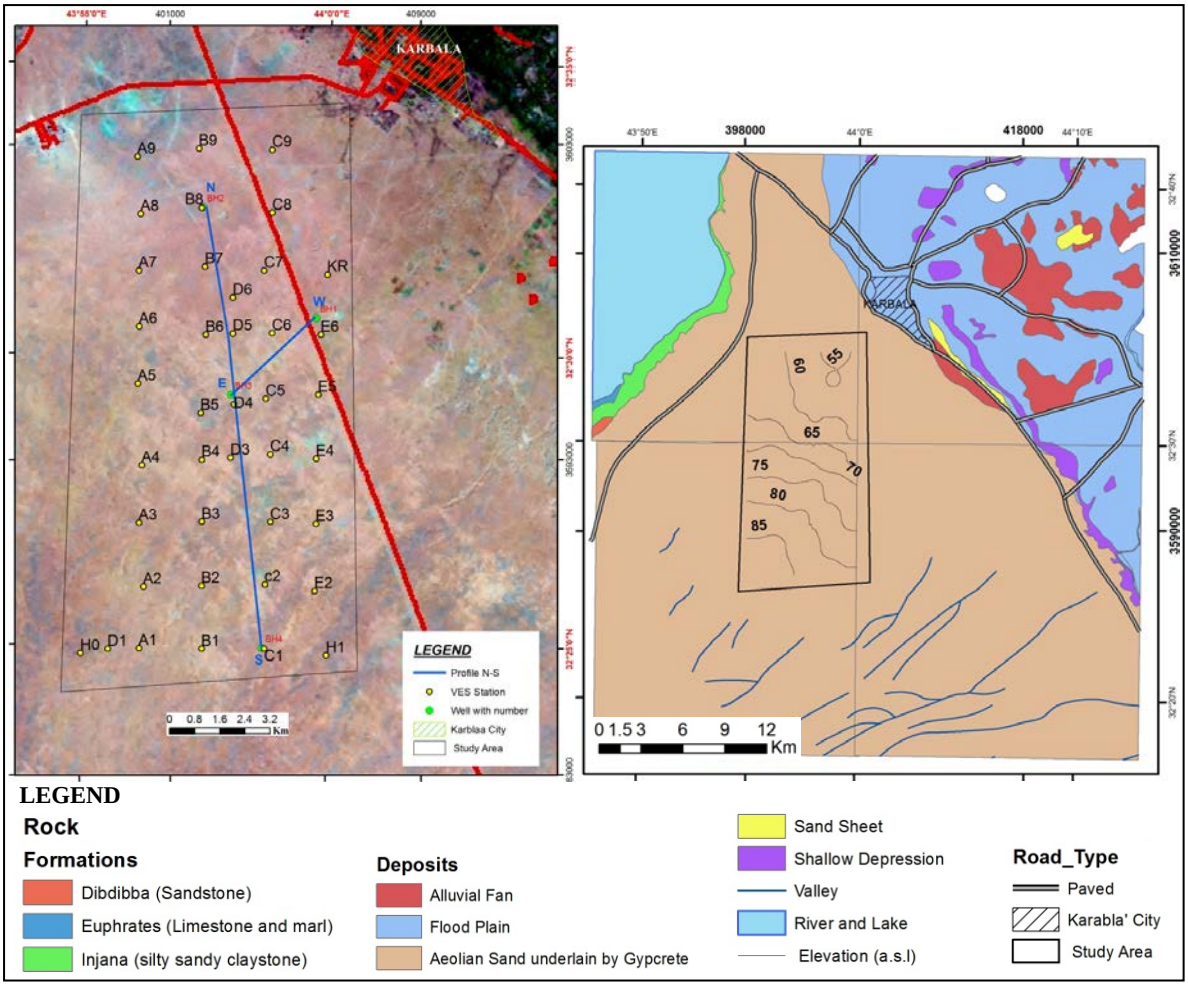


Fig.1: A Landsat satellite image (left) and the geological map (right) of the study area and surroundings, with contours of elevation (a.s.l.) and VES stations

- **Local Geology and Hydrogeology**

Tectonically, the location of the area is at the western margin of the Mesopotamia Foredeep Basin, within the vicinity of the northwest striking Abu Jir Fault system. The Cenozoic basin fill sequence typically consists of Paleogene open marine carbonates that grade into Neogene shallow water, lagoonal and restricted marine evaporite facies, overlain by deltaic and molasse clastic sediments (Fouad, 2010). The regional dip direction of the beds is to the northeast with dips ranging between 0° and 2° (Barwary and Slewa, 1995).

Injana Formation (Upper Miocene), which consists of silty sandy claystone, represents the main aquifer within the clastic sequence underlying the Dibdibba Formation (Pliocene – Pleistocene) (Al-Jiburi *et al*., 2012). Other formations, such as Euphrates, Fatha, Dibdibba and Quaternary west of Euphrates River are not considered as productive aquifers, although they may contain appreciable amounts of water, especially the Dibdibba and Euphrates formations when they become filled with water during the ephemeral wet seasons.

## ELECTRICAL RESISTIVITY MEASUREMENTS, INTERPRETATIONS AND RESULTS

Forty VES stations have been measured (Al-Bahadily *et al*., 2014). These stations are distributed along five N – S trending profiles, named A, B, C, D and E. The station spacing is approximately 2 Km (Fig.1).

Regularized 1D inversion modeling, constrained by the available geological information has been used to interpret the field curves with the aid of resistivity sounding interpretation software (IPI2Win, Version 3.0.1a) (Alexei *et al*., 2003). The inversion process is regularized by Tikhonov method whereby the observed data fit is constrained by 'priory' geological layer model. Resistivities and thicknesses as well as mismatch fitting errors are obtained for each model. The results show that 47% of the interpreted earth models are 5 layer cases and that 70% of the field curves can be interpreted by 3, 4 and 5 layer models.

The top layers are identified as aeolian sand underlying gypcrete bed. The interpretation shows that the gypcrete bed, which is characterized by relatively high resistivity, fits in nineteen stations' models. The median of the resistivity and the average thickness of the aeolian sand are 387 Ωm and 1.6 m, respectively, while they are 1140 Ωm and 2.13 m for the gypcrete. The average depth of the gypcrete is 1.6 m. This layer shows large variation in thickness and apparent resistivity depending on their occurrence form i.e. well crystallized, spongy and powdery form. The isopach distribution of the Holocene aeolian sands and the Pleistocene – Holocene gypcrete bed are presented as kriged grids over the study area in Figures (2) and (3), respectively.

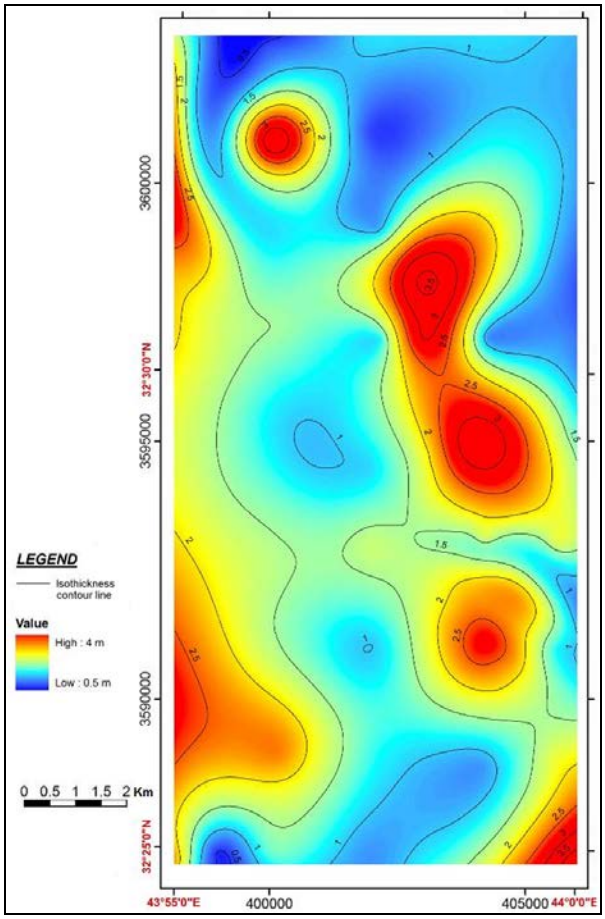


Fig.2: Isopach map of the aeolian sand in the study area (prepared by Kriging from VES data)

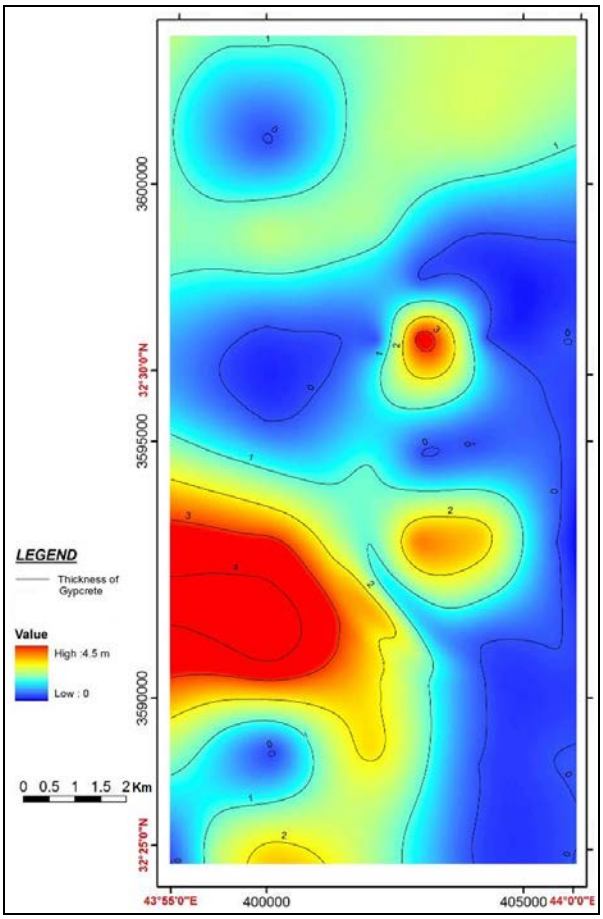


Fig.3: Isopach map of the gypcrete bed in the study area (prepared by Kriging from VES data)

- **Aquifer Determination**

An attempt to simplify the interpretation by assimilating the field curves into three groups instead of the wide range is suggested. This can be achieved by assuming the resistivity response of the aeolian sands and underlying gypcrete are treated as a single layer. This facilitates the interpretation of the first five electrical layers (which represent 70% of the earth models). The names of these groups, types of the field curves, frequency and percentage are presented in Table (1).

In consequence, the revised modeled resistivity, thickness, depth and anticipated geology of the electrical layers below the surface aeolian sand\ gypcrete layer are presented in Table (2) from which the main aquifer can be identified by its low resistivity that forms in four layers (layer 3, 4, 5, and 6) regrouped into three type curves. Figures 4 and 5 illustrate the typical field curves with their interpretations and with the low resistivity layer, assumed to represent the aquifer zone.

Table 1: Group names, types of field curves and percentage after consolidating the aeolian and gypcrete layers

| Group Name | VES Curve Type | Frequency | Percentage |
|---|---|---|---|
| QH | QH, QHK, KQH, KQHA, KQHK, KQHKH, KQH | 13 | 32.5 |
| HK | HK,HKQ, HKH,KHK, KHKH, KHKQ, KHKQH, KHKQQH, KHKHK | 18 | 45 |
| QQ | KQ, KQQ, KQQH, Q,QQHKH | 9 | 22.5 |
| **Total** | | **40** | **100** |

Table 2: The resistivity (ρ), thickness (h) and anticipated geology for the electrical layer underlying the aeolian sand and gypcrete bed

| Electrical Layer No. | ρ (Ω.m) Range/ Median | h (m) Range/ Average | HK Group | QH Group | QQ Group |
|---|---|---|---|---|---|
| **2** | 4.13 – 656/ 75 | 3 – 58/ 15.3 | Represents the upper part of Dibdiba Fn. friable sandstone. In many cases the sandstone is interbedded with claystone and treated as one electrical layer. The differences in h and the amount of water saturation have the main influence on the variation of ρ. | | Claystone |
| **3** | 1.0 – 1482/ 84.65 | 3.8 – 125/ 19.19 | Sandstone or dry claystone | | Claystone or the aquifer |
| **4** | 4594 – 2.0/ 32.55 | 11.3 – 70/ 31.3 | Marl or aquifer | Aquifer or Marl or limestone | Aquifer |
| **5** | 4664 – 2.0/ 18.1 | 17.1 – 39.3/ 20.8 | Marl or aquifer or limestone | | |
| **6** | 5.89 – 299/ 16.9 | 39.3 – 63.2/ 51.25 | Marl or aquifer or limestone | | |
| **7** | 2478 | – | Limestone | | |

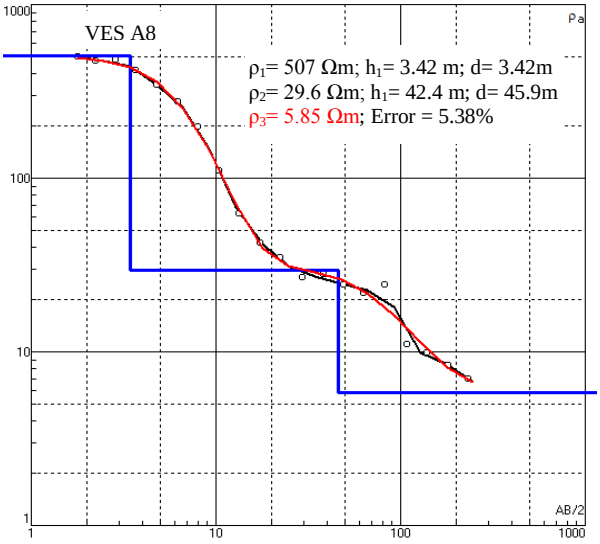


Fig.4: Interpretation of field curve of VES A8, the aquifer is defined as the third electrical layer with a modeled top contact depth of 45.9 m with $\rho_3$ = 5.85 Ωm

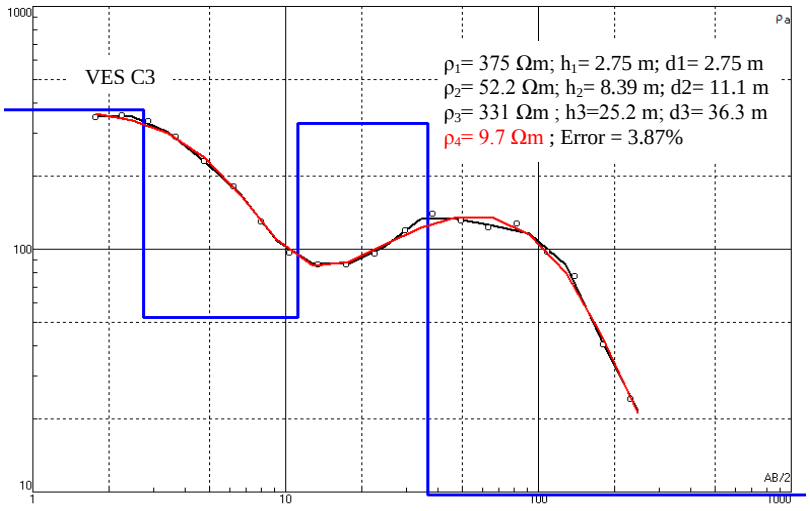


Fig.5: Interpretation of field curve of VES C3, the aquifer is the fourth electrical layer with a modelled top contact depth of 36.3 m with $\rho_4$ = 9.7 Ωm

Two maps have been constructed according to the results of the type curve model at each station; a depth to the top of the aquifer and resistivity of the aquifer as shown in Figs. (6 and 7). The depth to top may be directly compared to the current Hydrogeological Map of Iraq (Al-Jiburi and Al-Basrawi, 2015) and also with the hydrogeological map of Karbala Quadrangle (Al-Jiburi *et al.*, 2012). The maps compare well. However this new approach identifies a shallower depth contact of the aquifer in the northeast of the area (around 20 m) versus 40 – 50 m in the current hydrogeological maps of Karbala Quadrangle and Iraq.

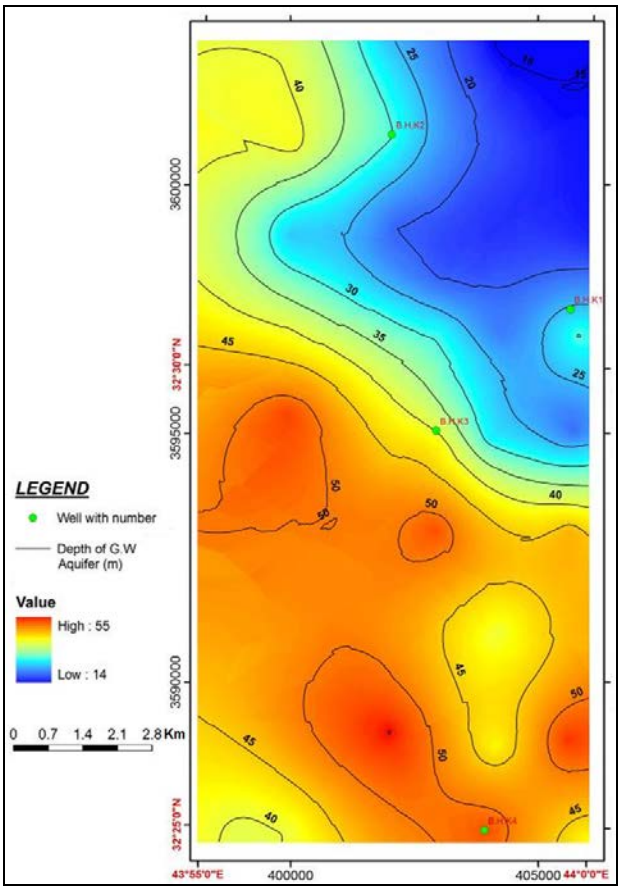


Fig.6: Depth to top of modelled aquifer (relative to sea level) in the study area

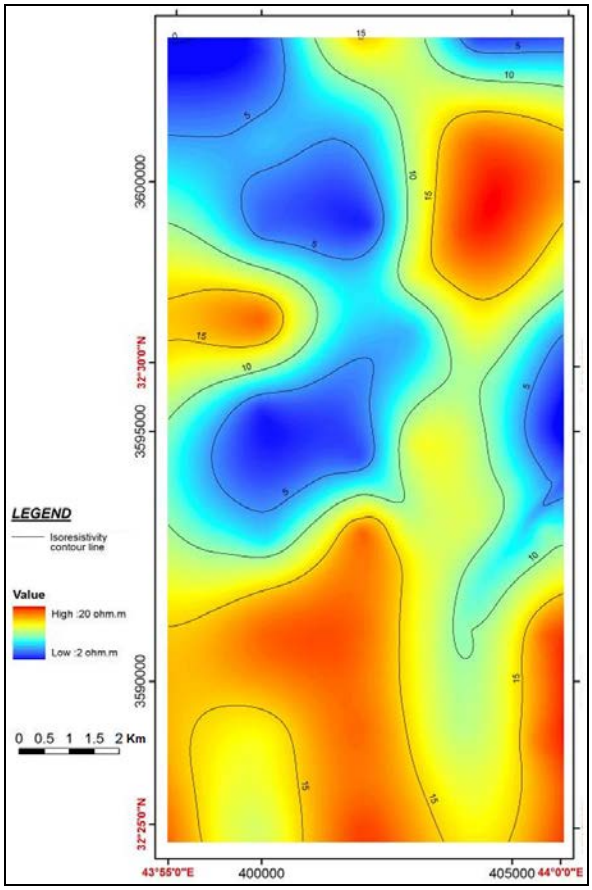


Fig.7: Isoresistivity map of the modelled aquifer layer in the study area

## ASSESSING THE ELECTRICAL ANISOTROPY OF THE OVERBURDEN

The electrical anisotropy coefficient ($\lambda$) is defined as the square root of the ratio of the resistivity measured perpendicular to the bedding ($\rho_T$) to that measured parallel to the bedding ($\rho_L$). It usually has a value between 1 and 2 (Sheriff, 1976).

$$\lambda = \sqrt{(\rho_T / \rho_L)}$$

For a geoelectrical column consisting of n electrical layers of unit square cross-sectional area (1 x l meter):

$\rho_T$ = the total transverse unit resistance (T)/ Total thickness (H) = $\sum \rho_1h_1+\rho_2h_2+\ldots..+\rho_nh_n$ /H

Where $\rho_1h_1$, $\rho_2h_2$ are the resistivity and thickness of the first and second layers

$$\rho_L = \text{Total thickness (H)/ Total longitudinal unit conductance (S)} = H/ \sum \rho_1/h_1+\rho_2/h_2+\ldots..+\rho_n/h_n$$

$$\text{The coefficient of anisotropy } (\lambda) = \sqrt{(\rho_T / \rho_L)} = (\sqrt{(T*S)})/ H$$

An assessment of the effect of varying the thickness and resistivity of a single model layer on the coefficient of anisotropy for the overburden sequence above the aquifer in the study area is now made. The coefficient of anisotropy is hence calculated for the entire geoelectrical column of model layers above the aquifer, given the model parameters for a

single station. Station VES B3 is selected on the basis of its total coefficient of electrical anisotropy model value (1.18 for the aquifer overburden sequence) being close to the ideal isotropic medium value (1). The ideal isotropic value represents a geoelectrical column in which there is no difference between transverse and longitudinal resistivity. Furthermore, the geoelectrical model for station VES B3 represents the most common configuration for the post-aquifer geological sequence in the study area. VES B3 is modelled with four electrical layers, which overly the aquifer, with a combined anisotropy coefficient value of 1.18.

Figure (8) firstly shows the effect of changing the thickness of the third layer, on the coefficient, λ. The figure shows that the maximum effect occurs when the layer thickness (h) because approximately one third of the total model thickness (H); that is 15 m thick and the anisotropy, λ is 1.21. The increment (Δλ) is relatively small (0.03).

Figure (9) shows the effect of changing the resistivity of the third layer ($\rho_3$) on the electrical anisotropy, λ. The anisotropy shows a large sensitivity to the resistivity when the value of $\rho_3 < 100$ Ωm (in other words, λ rapidly decreases with small increase in resistivity when the layer is highly conductive). The figure shows that the maximum effect occurs when the layer resistivity (ρ) is at its smallest, and the value of electrical anisotropy, λ in this case is 6.97. The increment (Δλ) is relatively high (5.79).

From the above discussion, considering that the survey is 1D in nature and assuming a horizontal and near isotropic layered earth model and considering that the interpreted resistivities and thicknesses are not different from their true values, it may be concluded:

The variation in thickness of any layer, within a geoelectrical column, the coefficient of anisotropy follows or may be expressed (best fitted) as a polynomial function of seven degree.
The λ is approximately constant at high thicknesses.
The effect of changing h on λ reaches a maxima when h = 1/3H with a sharp decay of anisotropy when h < 1/3H. Where h is the tested thickness, versus H, the total 'true' thickness.
The effect of varying the thickness of an electrical layer is relatively small in comparison to varying the layer's resistivity.
The variation in resistivity of any electrical layer, within a geoelectrical column, on the anisotropy follows or may be expressed (best fitted) as a polynomial function of the four degree.
The assumed water saturated clay bed or marls within a stratigraphic sequence increases the electrical medium's anisotropy.
The variation of λ suggests associated inhomogeneity in the sedimentary sequence and introduces uncertainty in depth estimation.

The electrical coefficient of anisotropy for the modelled overburden sequence is calculated for each VES station by using the total transverse resistance and total longitudinal conductance and the results are displayed in Fig. (10).

It follows that from the above Sheriff's definition, for isotropic sections $\rho_T = \rho_L$ and hence λ = 1. Anisotropic sections may generally be explained in a geologic context as possessing low resistivity parallel to the bedding (i.e. strike of the bedding planes) compared with that perpendicular to the bedding plane, where gradational changes in sedimentation are to be expected.

Figure (10) suggests that the bedding planes are essentially flat in the overlying sequence above the aquifer, in the central and southern portions, with good isotropic distribution. This is confirmed by the earlier measured bed dips.

Furthermore, Fig. (10) shows an east-west trend of high anisotropy in the northern half of the study area, which are suggested to be due to the presence of intervals of water saturated claystone, within the upper part of the geological sequence and below the Dibdibba Sandstone Formation.

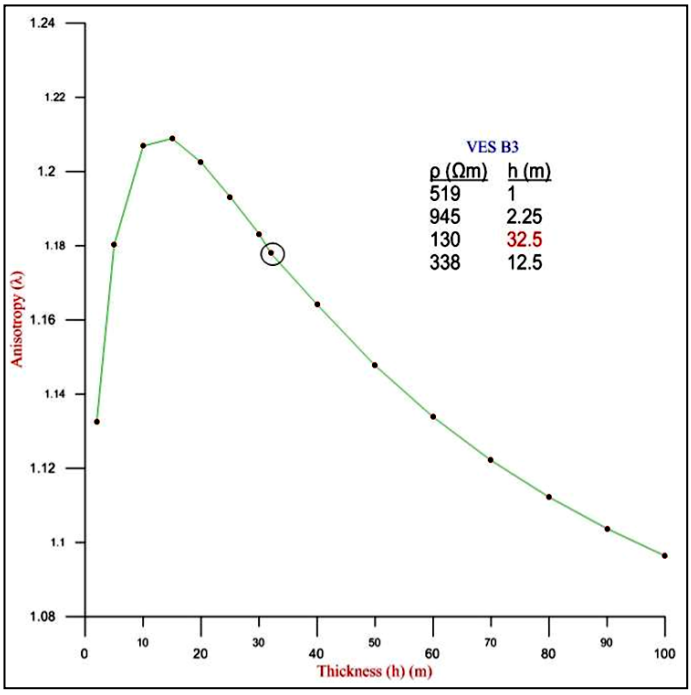


Fig.8: The anisotropy – thickness relationship. The maximum value of anisotropy (about 1.2) is encountered when the thickness of the tested layer (third layer) (h) = 1/3 total thickness (H). The "real" thickness of the tested layer is 32.5 m denoted by a circle on this curve

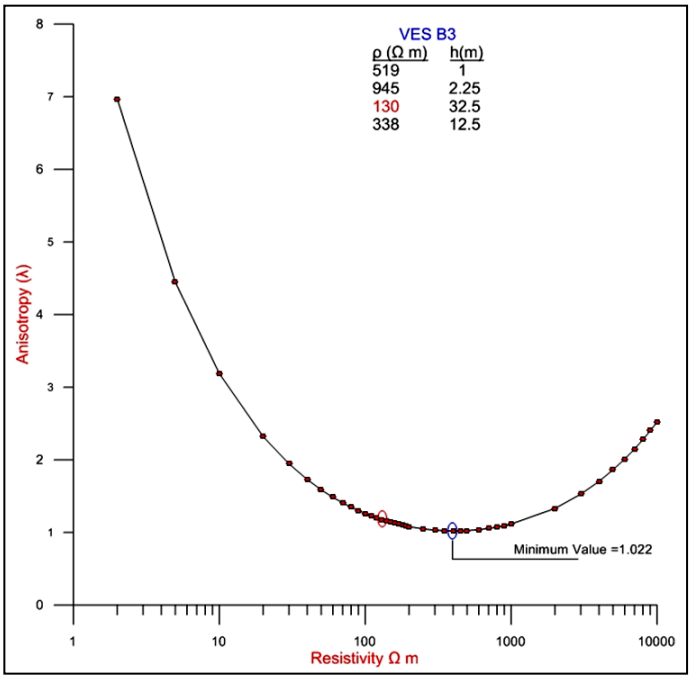


Fig.9: The anisotropy – resistivity relationship. The maximum value of anisotropy (6.97) is encountered when the resistivity of the tested layer (third layer) is 2 Ωm. The "real" resistivity of the tested layer is 130 Ωm denoted by a red circle on this curve. The lowest value of anisotropy (i.e. 'true' isotropic medium) is achieved when the resistivity is set to 400 Ωm denoted by a blue circle

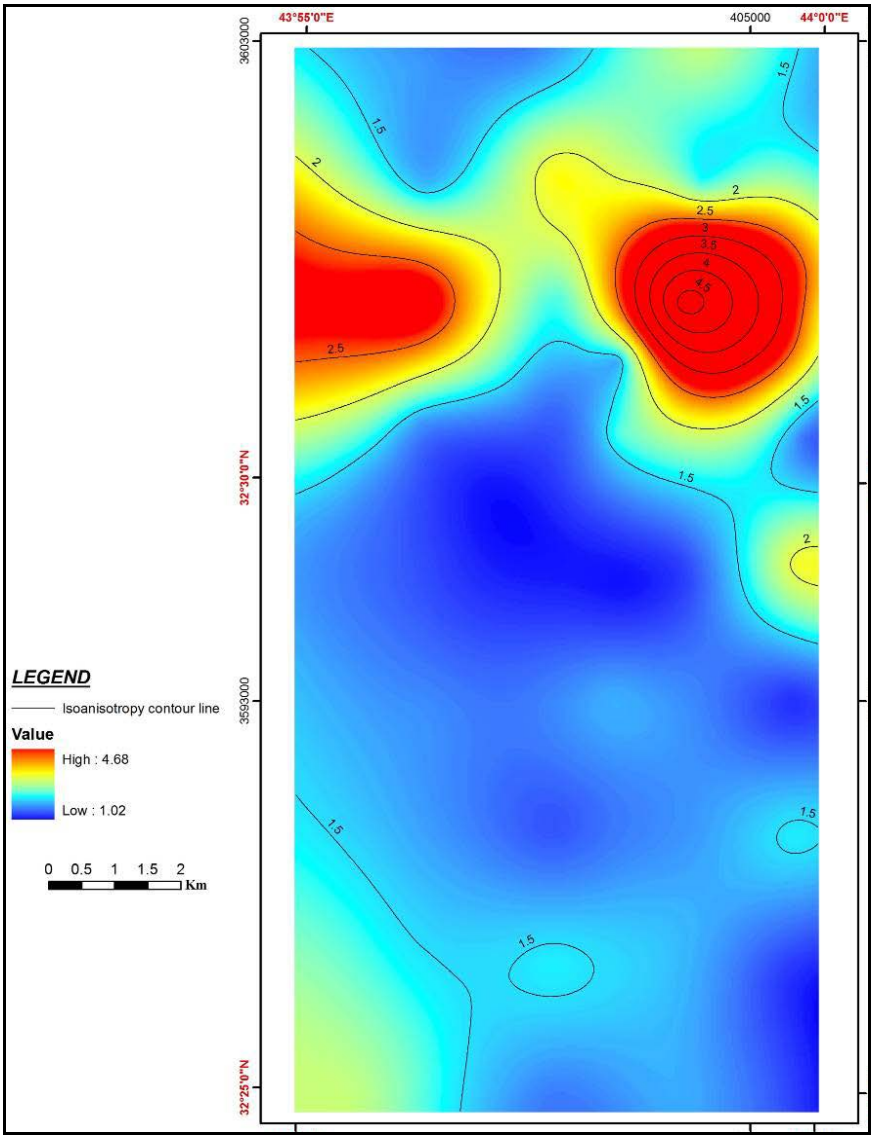


Fig.10: Map of anisotropy for the overburden sequence

## DRILLING INVESTIGATIONS

Following the interpretation, the wells BH1, BH2, BH3 and BH4 are drilled in the vicinity of VES stations E6, B8, D4 and C1, respectively (Alibdan, 2015) (Fig.1). The drilling report and the comparison of these results with the VES stations show lateral and vertical variations in lithology and thicknesses of the rock units reflecting the changes in the depositional environment throughout the area. The aeolian sand and the gypcrete bed are seen clearly in the VES model of station B8 and confirmed in BH2. The succession of sandstone and claystone behaves as a single electrical layer in the electrical column of these stations; with resistivity of 71 Ωm, 78.5 Ωm, 78.4 Ωm and 56.4 Ωm, respectively.

The aquifer is composed of silty sandstone and it is perfectly identified by the vertical electrical sounding. It is characterized by the low resistivity of 5.9 Ωm at depth of 36.8 m in BH1, and 13.7 Ωm at depth of 55.9 m in BH4. It is sandwiched between two impermeable beds, overlain by claystone and underlain by marl which suggests an aquifer of the confined

type. In addition, the claystone bed, which appears in VES station D4 at depth 9 m, has a resistivity value as low as that of the aquifer (4.45 Ωm). This is likely to be related to its saturation with water. Fence diagram, of these boreholes, is presented in Fig. (11) which shows the lithological variations.

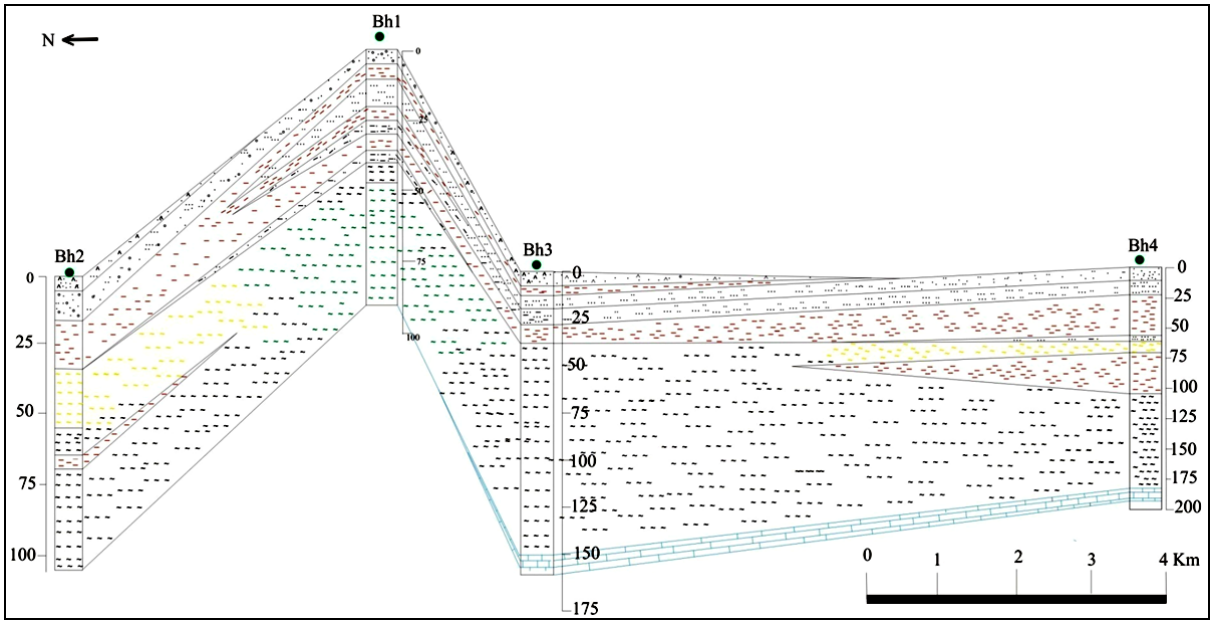


Fig.11: Fence diagram of the drilled boreholes showing the lithological variations. The aquifer, which is composed of silty sandstone, appears as a thin layer in Bh1 and Bh4

## GEOELECTRICAL CROSS-SECTIONS AND PRESENTATION

The pseudo and resistivity cross-sections in E – W and N – S directions are prepared (Figs.12 and 13). Pseudo E – W section (Fig.12a) shows two anomalies in the $\rho_a$; < 13.9 Ωm and > 373 Ωm at AB/2 about 12 m and 5 m. However, the $\rho_a$ of the aquifer is encountered at AB/2 170 m and 110 m; these are equivalent to depths of 46 m and 37 m, respectively, as shown in the inverted resistivity cross-sections (Fig.12b). The N – S pseudo section (Fig.13a), in VES D4, shows the effect of the low resistivity layer (saturated claystone at depth less than 10 m) of the penetrated depth, where the electrode separation can only overcome this effect when AB/2 being more than 20 m (Fig.13a and b).

The geoelectrical sections of these VES stations are presented in Fig. (14). The sections are prepared by the IPI2Win Program and compared with the drilling results. The figure shows the possibility of treating the clastic beds in the lithological profile as a single responsive electrical layer in the geoelectrical profile and conversely, dividing the claystone (and marl) beds into two electrical layers in the geoelectrical column (VES C1 at Bh4), given the resistivity response.

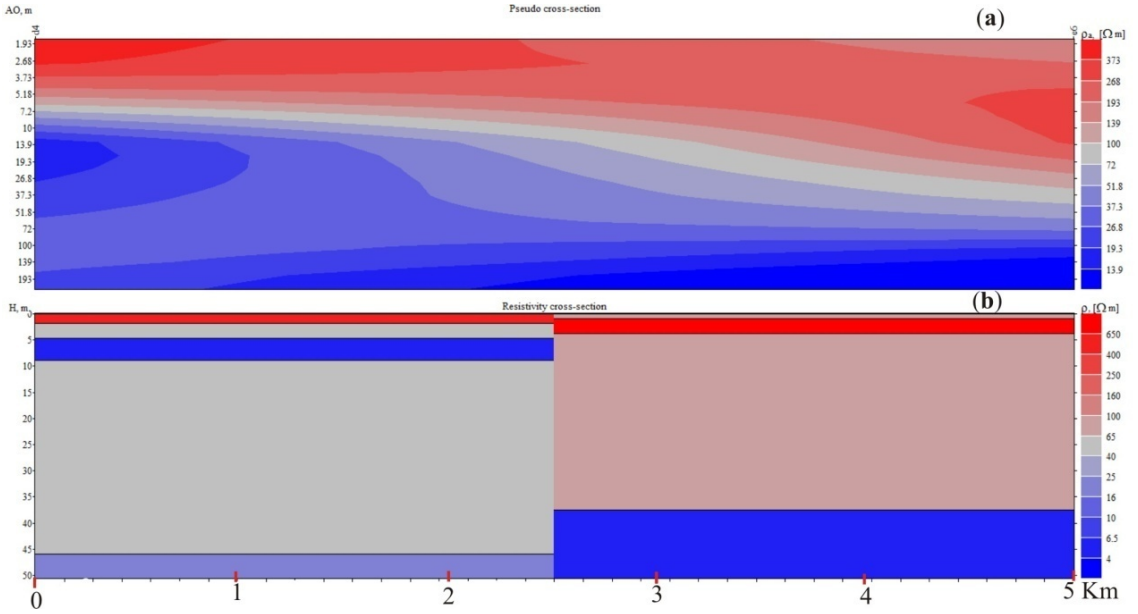


Fig.12: Pseudo (a) and resistivity (b) cross-sections in the E – W direction
(For location refer to Fig.1)

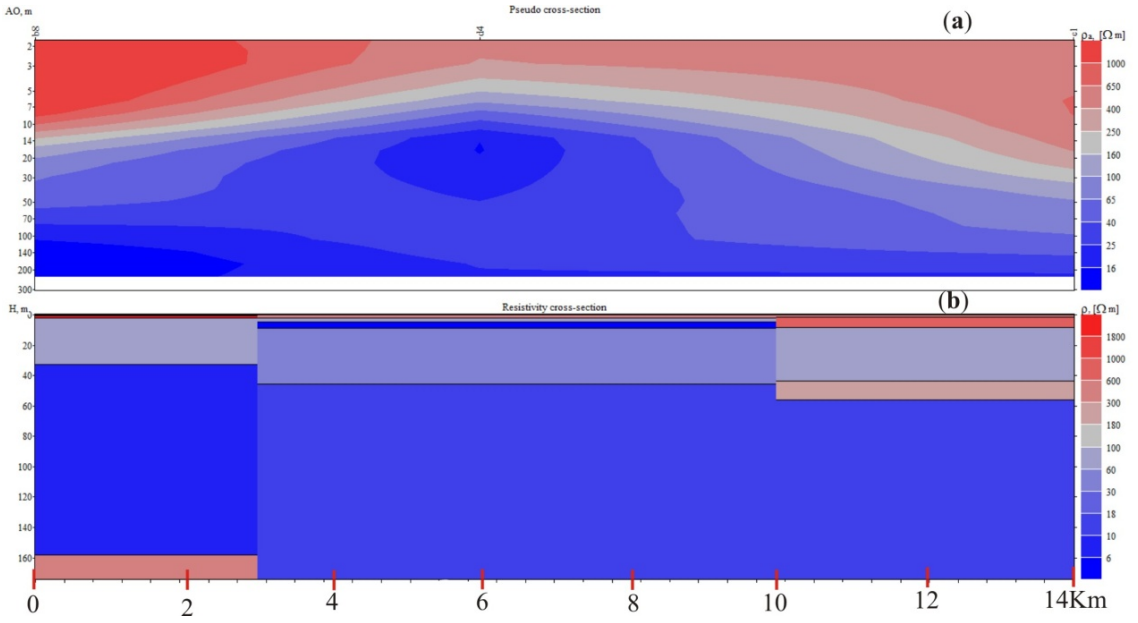


Fig.13: Pseudo (a) and resistivity (b) cross-sections in the N – S direction
(For location refer to Fig.1)

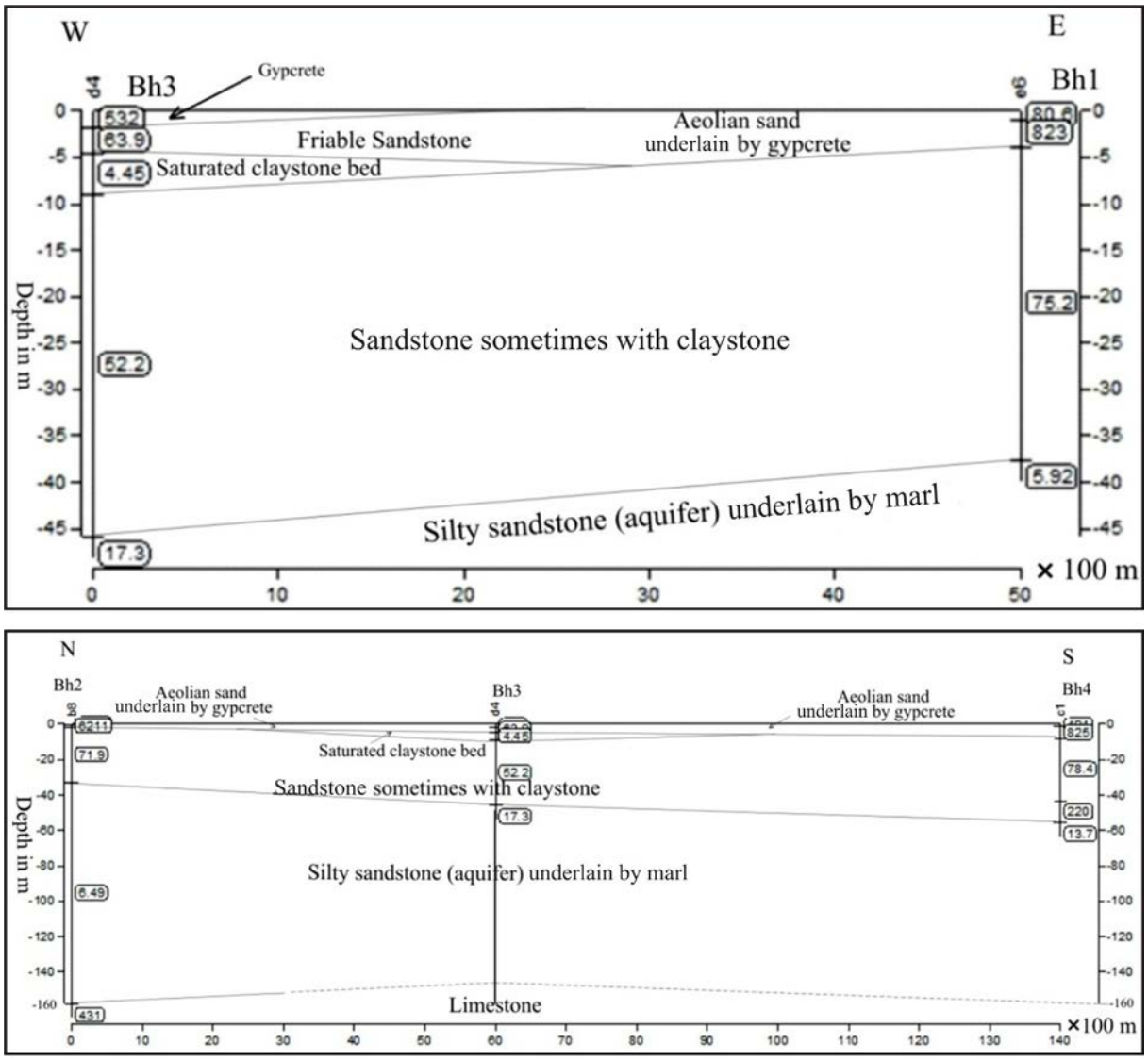


Fig.14: Geoelectrical cross-sections obtained by 1D interpretation of VES D4 and E6 in E – W direction (the upper) and B8, D4 and C1 in N – S direction (the lower)

## DISCUSSION AND CONCLUSIONS

The study of Abdul Qadir *et al*. (2013), in an area about 10 Km to the east of the present area, showed that groundwater aquifers in the Fatha and Dibdibba formations are polluted with hydrogen sulphide ($H_2S$) and oil. The transport path of the contamination must be along a structurally weak zone. They mentioned that subsurface fault movement may be in effect. The Neotectonic Map of Sissakian and Deikran (1998) indicates that the maximum subsidence in the Mesopotamia Basin is around 2500 m, measured from the top of exposed Fatha Formation (Middle Miocene). Local subsidence is estimated at 0 – 100 m from the same map. The authors consider the fault movement within the weak zone is responsible for the thickness variation of the sequences caused by the displacement and related subsidence. The variations in the measured electrical properties and consequently the interpreted earth models may support this fault displacement by the rapid changes observed in the modelled layer thicknesses. Accordingly, the geoelectrical models reflect the tectonic and structural disturbance in the area.

The isopach map of the aeolian sand (the top soil) (Fig.2) shows that the eastern and the western areas have greater thicknesses while the isopach map of the gypcrete bed (Fig.3) shows greater thickness in the mid-west part of the study area. By using these two maps, it is easy to delineate the best suited areas for agricultural development. Moreover, the areas free of gypcrete, which is almost impermeable, represent the rechargeable zones for upper open aquifer accumulations by direct rainfall infiltration. It should be mentioned that the lateral inhomogeneity in the resistivity of these two layers is related to rainy days. However, the variation of resistivity of gypcrete may also be attributed to the variations in its physical properties.

Ward (1983) states that overburden of irregular shape or resistivity will produce geologic noise which may render difficult the recognition of vertical variations in the resistivity profile of the "deep layers". Therefore, this lateral inhomogeneity may have a determining factor on the depth of investigation of the survey (which is 38.1 m for AB/2 = 233 m).

Also, lateral and vertical variations in lithology and thicknesses of the rock units reflect the changes in the depositional environment throughout the study area. Some of these variations, especially, when affected by water content, are reflected by the coefficient of anisotropy. The sensitivity analysis of this coefficient shows that the coefficient can be affected by lithological variation, (especially, for example, the water saturated claystone bed\ lenses), and more so than by lateral variation in the bed thickness. Both resistivity – anisotropy and thickness – anisotropy relationships follow a polynomial function.

The high anisotropy anomalies within the northern half of the area (Fig.10) may be attributed to the presence of water saturated claystones. It is believed that the absence of gypcrete (Fig.3) and the relatively low relief (Fig.1) have enabled rain water to collect and filtrate through the porous overlying sequence into the claystone unit.

The interpreted results indicate that the VES has provided a clear resistivity model of the aquifer; its depth, and lateral continuity. The results of drilling show that the central and southern parts of the study area have relatively good discharge factor (Q) and total dissolved salts (TDS).

The clastic succession, of Dibdibba and Injana formations, behaves as a single electrical layer in ten VES stations with average resistivity of 96 Ωm. The lower part of the claystone sequence which overlies the aquifer, is identified as an individual electrical layer in seventeen VES stations with an average resistivity of 176 Ωm. It is believed that this geophysical response is due to the dryness of this bed. However, the upper part of the claystones sequence, which has become water saturated by rain, exhibits a low resistivity response, with an average of 18 Ωm in ten VES stations, which is as similar as that recorded for the aquifer.

The results also indicate that the aquifer, which is composed of silty sandstone, of about 6 m thickness, has an average resistivity of 11.4 Ωm and average depth of 38.1m. In addition the marl bed which underlies the aquifer does not produce a resistivity contrast, where in many cases it behaves as a single resistive layer coupled with the aquifer. The recorded thicknesses of marl are 78 m and 122 m.

The electrode spacing which has been used in this survey is AB = 466 m. This has yielded an average investigation depth of 59 m and a median of 49.5 m (the depth to AB electrode spacing ratio is about 0.13). Although, the depths of the aquifer in BH1 and BH4 are

36 m and 56 m, respectively, and the aquifer has relatively small thickness, the electric current does not resolve the resistivity contrast at the bottom of the aquifer even when the distance of the current electrodes (AB/2) reaches the maximum separation of 233 m. This suggests that the resistivity of the marl is comparable to that of the aquifer, and hence there is no visible anomalous break in the resistivity.

## REFERENCES

Abdullahi1, M.G., Toriman, M.E. and Gasim, M.B., 2014. The Application of Vertical Electrical Sounding (VES) For Groundwater Exploration in Tudun Wada Kano State, Nigeria. International Journal of Engineering Research and Reviews; Vol.2, Issue 4, p. 51 – 55.

Abdul Qadir, S.O., Jawad, M.B. and Jassim, A.F., 2013. Geophysical methods supported by geochemical analysis to detect groundwater pollution in Karbala-Najaf area. GEOSURV, int. rep. no. 3460.

Alibdan, Kh.I.M., 2015. Geophysical and hydrological study for the area southwest of Karbala Governorate. GEOSURV, int. rep. no. 3541.

Al-Azzawi, A.S.M., 1997. Application of surface geoelectrical sounding method for estimating aquifer hydraulic properties in west of Samarra. Unpubl. M.ScThesis, Baghdad Univ., 102pp (in Arabic with English abstract).

Al-Bahadily, H.A., Abdul Qadir, S.O. and Al-Dujaily, A.F., 2014.Vertical electrical sounding for groundwater exploration southwest of Karbala city, Central Iraq. GEOSURV, int. rep. no. 3482.

Alexei, A.B., Igor, N.M. and Vladimir, A.Sh., 2003. IPIWin ver. 3.0.1a; User's Guide. Geoscan-M Ltd., Moscow, Russia, 2pp. (http://geophys.geol.msu.ru/ipi2win.htm).

Al-Jiburi, H.K. and Al-Basrawi, N.H. and Ibrahim, S.A.R., 2012. Hydrogeological and hydrochemical study of Karbala Quadrangle (NI-38-14), Scale 1: 250 000. GEOSURV, int. rep. no. 3364.

Al-Jiburi, H.K. and Al-Basrawi, N.H, 2015. Hydrogeological map of Iraq, scale 1: 1000 000, 2nd edition, Iraqi Bull. Geol. Min., Vol.11, No.1, p. 17 – 26.

Al-Khatib, A.A.Gh., 1988. Study of the geomorphology of Najaf Plateau. Unpubl. M.Sc Thesis, Baghdad Univ., 120pp. (in Arabic with English abstract)

Barwary, A.M. and Slewa, N.A., 1995. The Geology of Karbala Quadrangle (NH-38-6), scale 1: 250 000. GEOSURV, int. rep. no. 2318.

Fouad, S.F., 2010. Tectonic evolution of the Mesopotamia Foredeep in Iraq. Iraqi Bull. Geol. Min., Vol.6, No.2, p. 41 – 53.

Sissakian, V.K. and Deikran, D.B., 1998. Neotectonic Map of Iraq, scale 1: 1000 000, GEOSURV, Baghdad, Iraq.

Sheriff, R.E., 1976. Encyclopedic Dictionary of Exploration Geophysics, 3rd edit, Society of Exploration Geophysicists, Tulsa, Oklahoma, USA, 266pp.

Ward, S.H, 1983. Controlled source electrical methods for deep exploration. Geophysical Surveys 6, Dept. Geol. and Geophys., Univ. of Utah, D. Reidel Publishing Company, p. 137 – 152.

## About the Authors

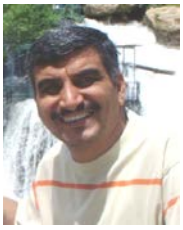

**Mr. Hayder A. Al-Bahadily,** graduated from University of Baghdad in 1994. He got his M.Sc. from the same university in 1997 in geophysics and joined GEOSURV in 1999. Currently, he is working as Chief Geophysicist in the Geophysics Department, GEOSURV. His main field of interest is applied geophysics. He has 30 documented reports and published papers.

**e-mail:** hayder.adnan17@gmail.com

**Mr. Sabah O. Abdulqadir,** graduated from University of Baghdad in 1979. He got his M.Sc. from the same university in 1984 in geophysics and joined GEOSURV in 1986. Currently, he is working as Senior Chief Geophysicist in the Geophysics Department, GEOSURV. His main field of interest is Electrical prospecting. He has 30 documented reports and published papers.

**e-mail:** sabahkirkuk@yahoo.com

**Mr. Andrew J. Long,** is a consultant geoscientist with over 15 years' experience working across different exploration sectors. Andrew graduated from Imperial College of the University of London with B.Sc. Geology with Geophysics 1997, and his M.Sc. Petroleum Geophysics in 1998. He started his career with PGS Reservoir as a consulting geophysicist. Andrew currently specializes in potential fields and geological integration and assists his clients with projects across Europe, Africa, Middle East and Central America. Andrew is a Fellow of the Geological Society of London and an active member of Society of Exploration Geophysicists.

**e-mail:** andrew.j.long.uk@gmail.com